Research on a Design Method of Generative Model for Cavity Section Shape of an Anechoic Coating

Yiping Sun [1, 2], Meng Tao [1, *]

[1] School of Mechanical Engineering, Guizhou University, Guiyang, China.

[2] Aviation Academy,Guizhou Vocational Technology Institute,Guiyang, China

* tomn_in@163.com

Abstract. One of the main challenges of the low frequency, broadband and strong sound absorption performance of an anechoic coating is the design of the cavity section shape. A generative-based design method was investigated in this study. Two generative-based models were trained to design the cavity section shape of anechoic coatings with a highly efficient absorption coefficient. The design results were compared in terms of mode collapse and average sound absorption coefficients. The results show that the WGAN-GP model can stably generate 100 new designs in only 3 seconds, dramatically speeding up the design process.

Keywords: structure; DCGAN; WGAN-GP; design.

1. Introduction

The underwater anechoic coating consists of a cavity and a substrate medium. A remarkable feature of the anechoic coating is the local resonance of the cavity. Early research mainly focused on the design of regular cavities in anechoic coatings [1-4]. The study on the absorption coefficients of these structures shows that the cavity geometry determines the lowest effective sound absorption frequency and bandwidth under the same material [5].

The acoustic characteristics of materials and structures are usually predicted using artificial neural networks [6][7]. The deep learning model with fine tuning super parameters has been used to automatic metasurface design [8]. Some generative models, such as variational autoencoders (VAEs) and generative adversarial networks (GANs), have been applied to complex heterogeneous composite reconstructions [9][10]. However, the generative model has not been published in the relevant literature in the structural topological design of underwater anechoic coatings.

In this study, the design model of underwater anechoic coating based on DCGAN and WGAN GP is studied and trained to learn the internal mapping between cavity section shape and acoustic performance. The generative model can creatively generate new data different from the original data. We use samples with average absorption coefficients in the range of 800 to 6000 Hz and greater than 0.75 as the data set, which includes 3000 images with a size of 128 pixels by 128 pixels [5]. The purpose is to obtain a topology with good sound absorption performance.

2. Modelling and analysis

2.1 The underwater anechoic coating model

The underwater anechoic coating is formed by embedding a cavity in a viscoelastic matrix medium. The actual size of the structure is referenced to be 14.17 mm by 14.17 mm [3]. Considering that an analytical solution is difficult to solve for irregular samples, in this paper, the sound absorption coefficients of the samples are calculated by FEM [5]. The numerical solution model is shown in Fig. 1(a). COMSOL Multiphysics 6.0 with MATLAB is used for the sweep frequency analysis of the periodic structure of the sound absorption coating.

Fig. 1(b) compares the absorption coefficient of a cylindrical cavity section shape calculated using numerical and analytical solutions. The consistency results within 6000 Hz prove that the FEM used in this paper is reliable.

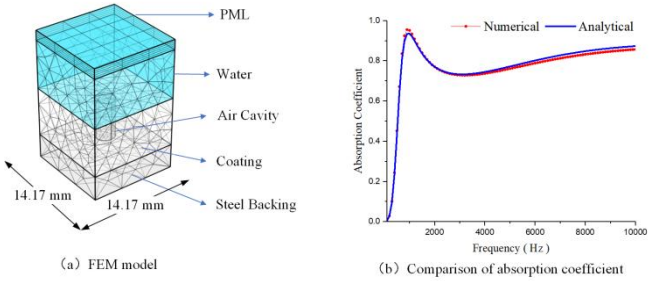

Fig. 1 Model analysis and solution.

2.2 Cavity section shape

In this paper, the coordinates (x1, x2) in (1) are used to solve the geometric contour of the cavity section shape [5]:

$$\begin{cases} x_1 = r_0 \left[1+\sum_{i=1}^{N} c_i \cos(n_i\theta)\right]\cos\theta \\ x_2 = r_0 \left[1+\sum_{i=1}^{N} c_i \cos(n_i\theta)\right]\sin\theta \end{cases} \tag{1}$$

The cavity section shape is constructed by the fourth order formula of (1). The parameters range are shown in Table 1, and r0 is equal to 1 mm.

Table 1. Range of parameters

Name	c1 ~ c4	n1 ~ n4
Min	0	0
Max	0.15	16

The high dimensionality of data is the difficulty in analyzing the sound absorption characteristics of irregular cavities [11]. Therefore, this paper studies a generation method of high-dimensional implicit mapping from sound absorption coefficients to cavity cross-section shape, which will be described in detail in Section III.

3. Generative-based Method

3.1 DCGAN-based model

The DCGAN model consists of a generator and a discriminator network. The generator maps random noise to fake coatings, while the discriminator innovatively discriminates the real and fake coatings. The workflow of training the DCGAN model for the anechoic coating feature reconstruction process is shown in Fig. 2(a), in contrast, the design part in Fig. 2(b) shows generation of the anechoic coating topologies.

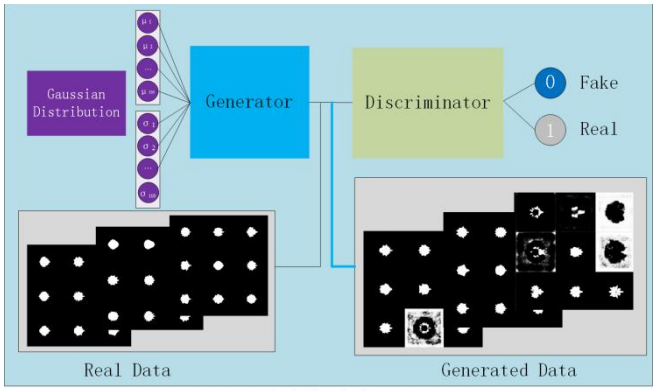

(a) Training

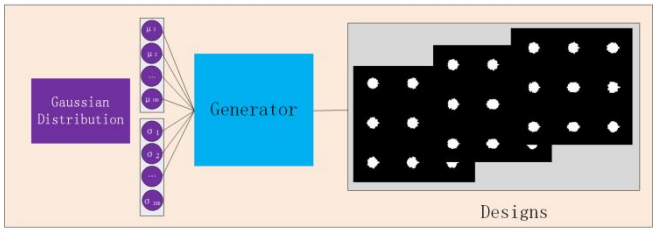

(b) Test

Fig. 2 Workflow diagram of DCGAN model.

The composition of the generator and discriminator can be described as follows: The input to the generator is a Gaussian distribution, which in this study contained 100 vectors, and the generator includes three transposed convolutional layers. Each transposed convolutional layer is followed by batch normalization and leaky ReLU activation, while the activation that followed the last layer is Tanh activation. The generator outputs a fake coating image. The discriminator has three convolution layers; each convolution layer is followed by batch normalization and leaky ReLU activation. The last layer outputs one neuron node, which discriminates whether the coating is legitimate.

The generator's goal is to generate a distribution as close as possible to the real data, while the purpose of the discriminator is to distinguish the generated data from the real data as much as possible. The similarity between the generated sample and the original sample depends on the antagonism of the model when DCGAN uses the "minimum maximum" loss function, which depends on the selection of weights. It forms a dynamic adversarial mechanism, and this dynamic countermeasure mechanism is improved through model training. The generator and discriminator continuously adjust the weight according to the loss value to update the gradient until the DCGAN model reaches Nash equilibrium [12]. Finally, a generator with a generating ability is obtained. The calculation process of "maximum and minimum" loss value based on DCGAN model is shown in (2).

$$\min_{G}\max_{D} V(\boldsymbol{D}, \boldsymbol{G}) = \mathrm{E}_{\boldsymbol{x}\sim p_{data}(\boldsymbol{x})}[\log \boldsymbol{D}(\boldsymbol{x})] + \mathrm{E}_{z\sim p_z(z)}[\log(1 - \boldsymbol{D}(\boldsymbol{G}(z)))] \tag{2}$$

Where D(x) represents the discriminator network when discriminating the generated and original coatings, G(z) represents the generator network when generating fake coatings based on a Normal distribution. Pdata(x) is the distribution of the original coatings, while Pz(z) is the distribution of the generated coatings.

3.2 WGAN-GP-based model

Training instability is a common problem with a DCGAN. The general practice is to train the discriminator with a dropout layer trick. Equation (2) is equivalent to minimizing the Jensen–Shannon (JS) divergence between Pdata(x) and Pz(z), as shown in (3).

$$JS(\boldsymbol{P}_{data} \parallel \boldsymbol{P}_z) = \frac{1}{2} KL(\boldsymbol{P}_{data} \parallel \frac{\boldsymbol{P}_{data} + \boldsymbol{P}_z}{2}) + \frac{1}{2} KL(\boldsymbol{P}_z \parallel \frac{\boldsymbol{P}_{data} + \boldsymbol{P}_z}{2}) \tag{3}$$

However, when the two distributions are completely disjoint at first, the final JS divergence is always log2, as shown in the yellow discriminator in Fig. 3. The model cannot converge, which leading to mode collapse.

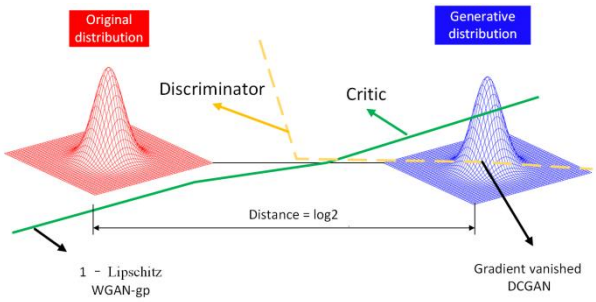

Fig. 3 JS divergence of two Gaussian distributions.

To make the training process more stable, a weight clipping strategy was adopted to forcibly satisfy the Lipschitz constraint on the discriminator based on the DCGAN, which is called the WGAN. However, careful design of the network and precise tuning of hyperparameters are needed to stabilize the training process. The loss function of the WGAN is shown in (4).

$$W(\boldsymbol{P}_{data}, \boldsymbol{P}_z) = \inf_{\gamma \sim \Pi(\boldsymbol{P}_{data}, \boldsymbol{P}_z)} \mathrm{E}_{(x,y)\sim\gamma}[\| x - y \|] \tag{4}$$

where W represents the Wasserstein distance between Pdata and Pz , x represents the original distribution, and y represents the generative distribution.

According to the Kantorovich–Rubinstein duality theory [13], when the discriminator satisfies the Lipschitz continuity condition, implemented by weight clipping, Equation (4) can be transformed into (5).

$$J^{(D)} = \mathrm{E}_{z\sim p_z}[f_w(G(z))] - \mathrm{E}_{x\sim p_{data}}[f_w(x)] \tag{5}$$

Where J(D) represents the discriminator loss value, and f is the critic, which is equivalent to the discriminator. The method of weight clipping to a specific range is too simple and crude; therefore, the loss function adds a gradient penalty to form the WGAN-GP, as shown in (6).

$$\min_G \max_D V(D, G) = \mathrm{E}_{z\sim p_z}[D(G(z))] - \mathrm{E}_{x\sim p_{data}}[D(x)] + \lambda \mathrm{E}_{x_s\sim p_{x_s}}[(\| \nabla_{x_s} D(x_s) \|_2 - 1)^2] \tag{6}$$

Where λ is a constant factor, and ∇_{x_s} is the gradient for randomly sampled values between the original distribution and the generated distribution.

The L2 norm size of the discriminator gradients in the WGAN-GP is constrained to be approximately 1 to satisfy the 1-Lipschiz continuous function. It can avoid gradient vanishing and solve the problem of non-convergence of the results when the two distributions do not disjoint, as shown in the green critic in Fig. 3.

4. Results and discussion

4.1 Results

The deep learning model of DCGAN and WGAN-GP is trained in an ordinary notebook computer, independently. The operating system is Windows10, the CPU is i5-8265U, the memory

is 8 GB and 2 GB NVIDIA independent graphics card. It is implemented on the Anaconda platform of Python 3.7 and trained using TensorFlow 2.0 framework. Figs. 4(a) and (b) show the generator and discriminator loss values of the two generative-based models in the training process, respectively. It can be seen from the comparison that under the condition of training for the same epoch, the discriminator loss value of the WGAN-GP is smaller than that of the DCGAN, which demonstrates the ability of the GP term to steer the generative distribution closer to the original distribution.

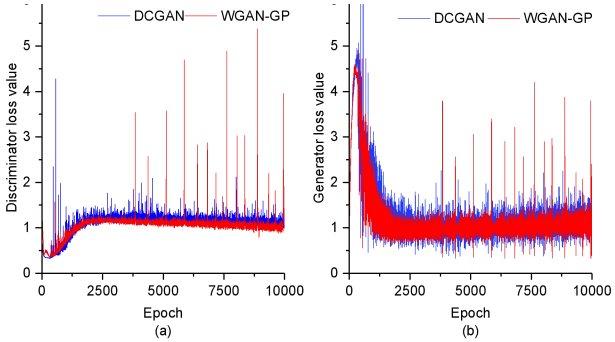

Fig. 4 Loss value of the two generative-based models.

The loss value of the DCGAN is obtained by finely designing the network. Under the condition of different configurations, the comparison of the generated coatings is shown in Fig. 5.

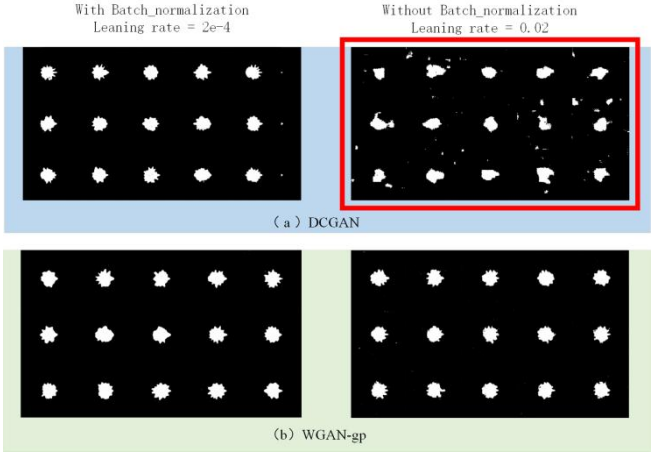

Fig. 5 Generated structures of the coatings. (a) DCGAN model with mode collapse, (b) WGAN-GP model without mode collapse.

Mode collapse occurs in the DCGAN without a batch normalization layer and a significant learning rate, as shown in Fig. 5(a), which demonstrating that DCGAN training is unstable and prone to mode collapse. Therefore, the WGAN-GP is more conducive to engineering applications, as shown in Fig 5(b).

4.2 Discussion

Based on the “Batchsize” processing capacity of WGAN-GP model, 100 cavity section shapes can be generated in 3 seconds. Using the trained model to generate a new design is hundreds of times more efficient than GA, which greatly speeds up the design process [14][15]. It should be noted that the process of WGAN-GP to generate a new cavity section shape completely follows the workflow of Fig. 2 and (6), and no prior knowledge is required. Numerical simulation verification has been carried out for the newly generated cavity section shape. The absorption coefficients corresponding to the eight randomly selected cavity section shapes are shown in Fig. 6.

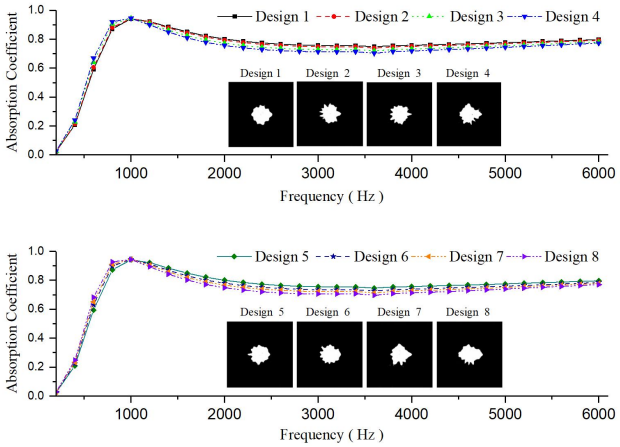

Fig. 6 Absorption coefficients of the generated designs.

The results show that the peak frequency corresponding to the cavity cross-section shape generated based on GAN is 1000 Hz, and the average absorption coefficient is greater than 0.7580 (800 Hz to 6000 Hz). The sound absorption effect of low frequency and broadband is realized.

Table 2. absorption effect of newly generated design

Design 1	Design 2	Design 3	Design 4
0.7963	0.7899	0.7748	0.7633
Design 5	Design 6	Design 7	Design 8
0.7952	0.7801	0.7707	0.7580

5. Conclusion

In this paper, a design method for cavity section shape of underwater anechoic coating based on GAN is studied, which realizes the cross application of cavity section shape design and depth learning. Compared with traditional methods, such as GAs, a GAN based method does not require real-time calculation, and can generate new data different from the training set. The WGAN-GP model is simple, efficient and more stable in the design of the cavity section of the low-frequency and broadband sound absorption coating. The results show that the interdisciplinary method based on deep learning has the immense potential in guiding mechanical structure design.

6. Acknowledgements

We would like to thank Gang Liu and other members of the materials team for helpful discussions. This work is supported by National Natural Science Foundation of China (52265010, 51765008); Science and Technology Project of Guizhou Province (2020-1Z048); Vocational Education Scientific Research Project of Guizhou Provincial Department of Education (GZZJ-Y2022011).

References

[1] Tang WL, He SP, Fan J (2005) Two-dimensional model for acoustic absorption of viscoelastic coating cylindrical holes. Acta Acoustic 30(4):289-295. https://doi.org/10.3321/j.issn:0371-0025.2005.04.001.

[2] Wang RQ. (2004) Methods to calculate an absorption coefficient of sound-absorber with cavity. Acta Acoustic 29(5):393-397. https://doi.org/10.3321/j.issn:0371-0025.2004.05.002.

[3] Tao M, Zhuo LK (2011) Effect of hydrostatic pressure on acoustic performance of sound absorption coating. Journal of Shanghai Jiao Tong University. 45(9):1340-1344+1350. https://doi.org/10.16183/j.cnki.jsjtu.2011.09.017.

[4] Tao M, Zhuo LK (2013) Acoustic performance of sound absorption coating containing composite cavities. Journal of Shanghai Jiao Tong University.47(3):408-412. https://doi.org/10.16183/j.cnki.jsjtu.2013.03.014s.

[5] Sun YP, Li ZY, Chen JD, Zhao XF, Tao M (2022) Variational autoencoder-based topological optimization of an anechoic coating: An efficient- and neural network-based design. Materials Today Communications 32:103901. https://doi.org/10.1016/j.mtcomm.2022.103901.

[6] Ciaburro G, Iannace G, Passaro J, Bifulco A, Marano AD, Guida M, Marulo F, Branda F (2020) Artificial neural network-based models for predicting the sound absorption coefficient of electrospun poly (vinyl pyrrolidone) / silica composite. Applied Acoustics 169(3):107472. https://doi.org/10.1016/j.apacoust.2020.107472.

[7] Sun YP, Bai Q, Zhao XF, Tao M (2022) Predicting the reflection coefficient of a viscoelastic coating containing a cylindrical cavity based on an artificial neural network model, Computer Modeling in Engineering & Sciences 130(2):1149-1170. https://doi.org/10.32604/cmes.2022.017760.

[8] Qiu TS, Shi X, Wang JF, Li YF, Qu SB, Cheng Q, Cui TJ, Sui S (2019) Deep learning: a rapid and efficient route to automatic metasurface design. Advanced Science 6(12):900128. https://doi.org/10.1002/advs.201900128.

[9] Cang RJ, Li HC, Yao HP, Jiao Y, Ren Y (2017) Improving direct physical properties prediction of heterogeneous materials from imaging data via convolutional neural network and a morphology-aware generative model. Computational Materials Science 150:212-221. https://doi.org/10.1016/j.commatsci.2018.03.074.

[10] Yang ZJ, Li XL, Brinson C, Choudhary A, Chen W, Agrawal A (2018) Microstructural materials design via deep adversarial learning methodology. Journal of Mechanical Design 140(11):111416. https://doi.org/10.1115/1.4041371.

[11] Bessa MA, Bostanabad R, Liu Z, Hu A, Apley DW, Brinson C, Chen W, Liu WK (2017) A framework for data-driven analysis of materials under uncertainty: countering the curse of dimensionality. Computer Methods in Applied Mechanics and Engineering 320(15):633-667. https://doi.org/10.1016/j.cma.2017.03.037.

[12] Radford A, Metz L, Chintala S (2016). Unsupervised representation learning with deep convolutional generative adversarial networks. Computer ence. https://doi.org/10.48550/arXiv.1511.06434.s

[13] Argyros IK, Hilout S (2014). The majorant method in the theory of newton–kantorovich approximations and generalized lipschitz conditions. Journal of Computational and Applied Mathematics 291:332-347. https://doi.org/10.1016/j.cam.2014.12.013.

[14] Tao M, Wang GW (2013) Parameter optimization of a sound absorption layer based on multi-objective genetic algorithm. Journal of Shanghai Jiao Tong University 47(8):1300-1305. https://doi.org/10.16183/j.cnki.jsjtu.2013.08.023.

[15] Tao M, Zhao Y, Wang GW (2014) Parameter optimization of sound absorption layer based on genetic algorithm. Journal of Vibration and Shock 33(2):20-25. https://doi.org/10.13465/j.cnki.jvs.2014.02.031.